

RESEARCH ARTICLE

Potential-Game-Based 5G RAN Slice Planning for GBR Services

OSCAR ADAMUZ-HINOJOSA^{ID}, PABLO MUÑOZ^{ID},
PABLO AMEIGEIRAS^{ID}, AND JUAN M. LOPEZ-SOLER^{ID}

Department of Signal Theory, Telematics and Communications, University of Granada, 18014 Granada, Spain

Corresponding author: Oscar Adamuz-Hinojosa (oadamuz@ugr.es)

This work was supported in part by the H2020 Research and Innovation Project Beyond 5G Multi-Tenant Private Networks Integrating Cellular, Wi-Fi, and LiFi, Powered by Artificial Intelligence and Intent Based Policy (5G-CLARITY) under Grant 871428, in part by the Spanish Ministry of Economy and Competitiveness, and in part by the European Regional Development Fund under Project PID2019-108713RB-C53, and in part by the Spanish Ministry of Economic Affairs and Digital Transformation under Project TSI-063000-2021-28.

ABSTRACT The Radio Access Network (RAN) slice planning is a key phase within the RAN slice management and orchestration process. Based on the performance requirements of requested RAN slices and key performance indicators of the RAN and existing RAN slices, the RAN slice planning mainly consists of deciding (a) the feasibility of deploying new RAN slices; (b) re-configuring the existing RAN accordingly; and (c) the need to renegotiate the Service Level Agreements (SLAs) and/or expand the RAN (i.e., radio resources, carriers, cells etc) if one or more RAN slices cannot be accommodated in a first attempt. Under this context, we propose a framework for planning RAN slices which require their data sessions get a Guaranteed Bit Rate (GBR) and the probability of blocking such sessions is below a threshold. To meet such requirements, our framework plans the amount of prioritized radio resources for new and already deployed RAN slices. We formulate the RAN slice planning as multiple ordinal potential games and demonstrate the existence of a Nash Equilibrium solution which minimizes the average probability of blocking data sessions for all the RAN slices. We perform detailed simulations to demonstrate the effectiveness of the proposed solution in terms of performance, and renegotiation capability.

INDEX TERMS Blocking probability, game theory, GBR services, radio resource allocation, RAN slicing planning.

I. INTRODUCTION

Radio Access Network (RAN) slicing is one of the key technologies for 5th generation (5G) mobile networks [1]. It consists of providing logically separated RANs, denominated RAN slices, each tailored to the requirements of a specific communication service over a common infrastructure. The 3rd Generation Partnership Project (3GPP) has identified four phases for the lifecycle management of a RAN slice: preparation, commissioning, operation and decommissioning [2]. In the preparation phase, the Mobile Network Operator (MNO) performs: the design and capacity planning of incoming RAN slices; the network environment prepa-

ration; and the on-boarding and evaluation of RAN slice's constituents for testing purposes.

In this paper we focus on the RAN slice planning, which is a procedure within the preparation phase [3]. This procedure takes as inputs (i) the performance requirements of one or more requested RAN slices and (ii) statistics of key performance indicators of the RAN and the already activated RAN slices. Based on these inputs, the RAN slice planning aims to decide in advance: (a) the feasibility of deploying the requested RAN slices; (b) the adequate parameter configuration of the RAN to accommodate their spatio-temporal traffic demands; and (c) the need to renegotiate the Service Level Agreement (SLA) and/or expand the RAN (i.e., radio resources, carriers, cells etc) if the RAN slices cannot be accommodated in a first attempt.

The associate editor coordinating the review of this manuscript and approving it for publication was Jad Nasreddine^{ID}.

In practice, two or more RAN slices may coexist in time. In such case, the MNO could benefit from a joint planning of these RAN slices (e.g., optimizing the resource utilization). For this reason, since the MNO receives the RAN slice requests in advance, we assume the RAN slice planning can be executed in multiple time windows, and for each window, it may process more than one RAN slice request. The duration of the time window mainly depends on how frequently the MNO receives RAN slice requests, e.g., from several hours, to several days, or even weeks.

Although the RAN slice planning is necessary for the RAN slice management and orchestration, it has barely been researched in the literature. There exist solutions which address the cell planning [4], [5] and spectrum sharing strategies [6], [7]. Specifically, they mainly focus on the deployment of the RAN infrastructure, in greenfield scenarios, considering RAN slicing. However, it differs from the RAN slice planning, where the existing RAN infrastructure and RAN slices impose constraints on planning the requested RAN slices. Recently, the authors of [8] have proposed a solution to reserve infrastructure resources throughout different planning windows to multiple network slices. Despite their valuable contribution, they omit the radio channel model and how it impacts the translation from the RAN slice requirements into the amount of radio resource which meet such requirements.

Instead of RAN slice planning, most of the state-of-the-art proposals focus on a slightly different procedure known as admission control. In this problem, the MNO typically processes one-by-one RAN slice requests for immediate deployment. Then, for each request, the MNO verifies the feasibility of deploying the corresponding RAN slice under the current traffic conditions. If feasible, the RAN slice is immediately deployed. Otherwise, the RAN slice is rejected without considering any SLA renegotiation and/or expansion of the RAN infrastructure to accommodate it.

Representative solutions for the admission control are [9], [10], [11], [12], where the authors propose mechanisms to allocate radio resources to the requested RAN slices. These solutions mainly focus on the system dynamics (i.e., dynamic admission and rejection of several RAN slices) throughout the time, e.g., by analyzing the rate of rejected RAN slices, resource utilization, etc. However, these solutions cannot be applied for planning RAN slices because they do not permit SLA renegotiation and/or network expansion. Additionally, although some solutions, e.g., [10], [12], consider the MNO can simultaneously process more than one RAN slice request, they are not valid for planning because they omit how the channel effects impact the translation from performance requirements into radio resources. Finally, some of these solutions do not consider the expected data session creation/release of each requested RAN slice.

In this paper, we propose a mathematical framework, denominated RAN Slice Planner, to plan in advance requested RAN slices over an existing RAN infrastructure. We consider each individual RAN slice demands the follow-

ing requirements: (a) each User Equipment (UE) session must get the Guaranteed Bit Rate (GBR) specified in the SLA; and (b) the probability of blocking a UE session must be below a threshold. Based on such requirements, the RAN Slice Planner decides the adequate parameter configuration of the RAN. Particularly, our framework establishes the minimum amount of prioritized radio resources¹ which will meet such requirements for the busy hour. Hereinafter, we refer to the amount of prioritized radio resources per RAN slice in each cell as radio resource quota. Under this context, the specific contributions of this paper are:

- We provide a step-by-step description about (a) the stages and the key aspects that the MNO must consider to plan multiple RAN slices, and (b) the integration of the RAN slice planning within the well-known 3GPP-based RAN slicing management framework.
- We formulate the RAN slice planning problem as the establishment of radio resource quotas while the average UE blocking probability for all the RAN slices is minimized. It is a combinatorial and non-convex problem with at least NP-hard complexity. For this reason, we adopt game theory to find a local optimum, i.e., a Nash Equilibrium (NE) solution [13]. Specifically, we model our problem as multiple ordinal potential games and design novel strategies based on better response dynamics to solve it.
- We illustrate the benefits of the RAN Slice Planner in an scenario with resource scarcity. Particularly, we show how our solution performs SLA renegotiation to accommodate all the requested RAN slices over an existing RAN infrastructure.

The remainder of this paper is organized as follows. Section II provides the related works. Section III sheds light on the RAN slice planning under the 3GPP RAN slice management framework. Section IV describes the system model. In Section V, we formulate our problem as multiple ordinal potential games. Section VI describes the proposed strategies for RAN slicing planning. Section VII evaluates the performance and the renegotiation capability of our solution. Finally, Section VIII summarizes the conclusions and provides some outlooks for future work.

II. RELATED WORKS

Most of the state-of-the-art proposals which study the feasibility of deploying RAN slices focus on the admission control problem. Examples can be found in [14], [9], [15], [10], [16], [11], and [12]. In such works, the authors typically assume the MNO receives requests for deploying RAN slices following a Poisson distribution. They assume an exponential distribution for the lifetime of each RAN slice. Furthermore, for each individual RAN slice, they typically consider a fixed amount

¹Prioritized radio resources are those which are guaranteed for a single RAN slice (e.g., slice A), but they may be used by other RAN slices (e.g., slices B and C) if the corresponding RAN slice (i.e., slice A) do not need them at any time.

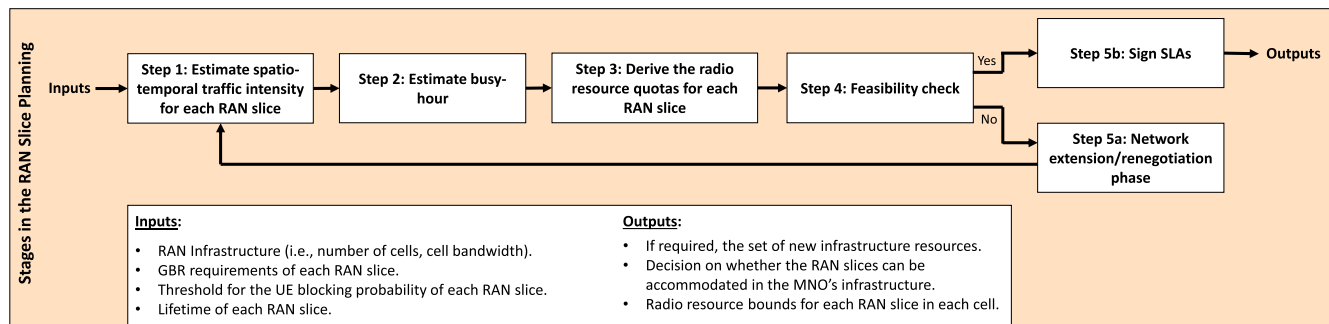


FIGURE 1. Description of the steps performed in the RAN slice planning. Note that the described inputs and outputs are adapted to RAN slices with GBR requirements.

of UEs consuming GBR services. Based on these assumptions, the authors model the system by queuing theory-based models and/or Markov chains. Then, they use these models to analyze the performance of the admission control, i.e., rate of rejected RAN slices, resource utilization, etc.

Despite their valuable contributions, the existing solutions on admission control present some limitations which prevent the MNO to use them as planning tools. In [9], [15], [10], [16], [11], and [12], the proposed solutions assume that unfeasible RAN slice requests are immediately rejected instead of executing SLA renegotiation and/or network expansion procedures. Other works as [10], [16], and [12] consider the admission control can simultaneously process more than one RAN slice request in a planning window. However, these solutions consider a generic definition of resource instead of radio resource. This means these solutions do not consider how the channel effects impact the translation from performance requirements into radio resource quotas.

The previous solutions check the feasibility of deploying RAN slices from an admission control viewpoint. From a RAN slice planning perspective, the literature is scarce. Works such as [17] and [18] address the network slice planning considering only the core network. Focusing on RAN, there exists works such as [4] and [5] which address the cell planning considering a multi-tenant environment, and others as [6] and [7] which analyze spectrum sharing strategies for different RAN slices. These solutions focus on the deployment of a new RAN infrastructure considering RAN slicing. Instead of that, we consider an existing RAN infrastructure with running RAN slices and how it constrains the planning of new RAN slices. In [8], the authors have proposed a solution to reserve infrastructure resources throughout different planning windows. Specifically, it aims to minimize the cost of reserving infrastructure resources from the MNO perspective. Despite its value, this solution does not consider neither the UE blocking probability as a RAN slice requirement nor the dynamic creation/release of GBR sessions for a RAN slice. Additionally, the authors of [8] focus on planning the Virtual Network Functions (VNFs) and Service Function Chains (SFCs) of the requested network slices instead of planning their radio resources.

Focusing on GBR services, works such as [19] and [20] provides novel solutions to allocate radio resources among UEs served by different RAN slices, each with specific GBR requirements. These proposals assume the UE data sessions could consume more data rate than the GBR. This overuse of the available radio resources may prevent more data sessions of the same slice could be admitted. In our proposal, we assume each UE just consumes the GBR defined in the SLA. Some of these works have also evaluated the UE blocking probability for each RAN slice. To that end, they have modeled the UE session generation and release by a Markov process. This means these solutions must assume an exponential distribution for the UE session duration. In our work, we go beyond by considering generic distributions for the UE session duration.

Game theory has been widely used for modeling the radio resource allocation in RAN slicing. In [21], the authors use a weighted congestion game to perform user-cell association and distribute the available radio resources among several tenants based on the level of their financial contribution to the wireless network infrastructure. In [9], [22], and [23], the same authors use Fisher market to model the radio resource allocation for non-GBR and GBR RAN slices. Unlike our proposal, their solutions do not guarantee the UE blocking probability for each RAN slice in each cell is below a certain upper bound. In [24], the authors use matching theory to address the radio resource allocation in RAN slicing. Despite its valuable contributions, this work does not consider the impact of inter-cell interference levels and the establishment of an upper bound for the UE blocking probability.

Finally, there exist solutions based on potential games to allocate radio resources. For instance, the authors of [25] have proposed a mathematical framework based on potential games to address the radio resource allocation problem in several scenarios such as smart-grid networks, or networks with relay nodes. In [26], the authors have formulated with a potential game the co-channel interference coordination problem in a heterogeneous network where device-to-device users, macro cell users, and micro cell users coexist. Despite their valuable contributions, these works do not consider

RAN slicing, i.e., guaranteeing performance isolation among different services.

III. PLANNING RAN SLICES WITH THE 3GPP RAN SLICE MANAGEMENT FRAMEWORK

In this section, we first describe the steps the MNO must perform during the RAN slice planning. Then, we elucidate the procedures carried out by the 3GPP RAN slice management framework—in the context of RAN slice planning—from the communication service requests to the establishment of the radio resource quotas.

A. STAGES IN THE RAN SLICE PLANNING

We assume the MNO considers periodical time windows where new RAN slices may be deployed. For each time window, the MNO executes in advance a planning procedure which aims to accommodate the requested RAN slices along with the existing ones in its infrastructure.

Considering a single time window, we illustrate a potential realization of the planning procedure for multiple RAN slices in Fig. 1. The MNO takes as inputs the performance requirements of all the RAN slices and the information about its RAN infrastructure. In turn, the outputs are: (a) the amount of RAN slices which can be accommodated; (b) if required, the new infrastructure resources which would be deployed before instantiating the requested RAN slices; and (c) the configuration of the RAN infrastructure which includes, among other things, the radio resource quotas.

To obtain these outputs, the MNO must translate the performance requirements of each RAN slice into RAN resources. To that end, the MNO needs first to estimate the spatio-temporal traffic intensity experienced by each RAN slice in the considered time window (step 1). With this information, the MNO can determine the busy hour (step 2), i.e., the time period when the RAN infrastructure suffers the worst-case inter-cell interference.

Considering the busy hour, the MNO derives the amount of radio resources required by each RAN slice in each cell (step 3). The MNO then checks if the performance requirements of all the RAN slices are met with such allocation (step 4). If the checking procedure fails, a network extension/renegotiation phase starts (step 5a). In this phase, the MNO should consider at least one of the following options: (a) adding more radio resources to the RAN infrastructure; (b) renegotiating the SLAs with one or more tenants; or (c) rejecting the least attractive RAN slices based on a metric. This phase ends when a successful checking procedure is reached, and both the MNO and every tenant sign the SLAs (step 5b). As a result, the MNO uses the radio resource allocation performed in the checking procedure to determine the radio resource quotas.

In this work, we focus on the steps 3-5 depicted in Fig. 1. The estimation of the spatio-temporal traffic demands of each RAN slice (step 1) and the busy hour for a planning window (step 2) would deserve further investigation but is beyond the scope of this work.

B. FROM SERVICE REQUESTS TO THE ESTABLISHMENT OF THE RADIO RESOURCE QUOTAS

To compute the radio resource quotas for the requested RAN slices and recompute them for the existing RAN slices, the MNO must rely on the well-known RAN slicing framework depicted in Fig. 2. The main entities and mechanisms of this framework have already been standardized by leading Standards Developing Organizations (SDOs) on RAN slicing such as the 3GPP and the Global System for Mobile Communications Association (GSMA) [28], [29]. Furthermore, several proposals from the literature such as [30], [31], [32], [1] have provided novel contributions on RAN slice management based on this framework. In this section, we shed light on how the RAN slice planning must be integrated in this framework.

At the beginning of a planning period, the MNO must process the deployment requests for one or more communications services. At this point, it is crucial for the MNO to define a mechanism to (a) interpret the requirements from different tenants, and (b) represent them in a common language. In this regard, the GSMA has developed a universal network slice blueprint that provides a point of convergence between the MNO and the tenants on network slicing understanding. This blueprint, known as *Generic Network Slice Template (GST)*, contains a set of attributes that can be used to characterize the communication service to be accommodated by a network slice [29], [33].

Focusing on Fig. 2, we assume the tenants have available the GST's attributes to set them in a customized way (step 1). Alternatively, these attributes could be totally or partially set by the MNO. In any case, when all the attributes are set (step 2), the requirements of a specific communication service are gathered in the *Network Slice Type (NEST)*. Different NESTs allow describing different types of network slices, which are registered and published in the MNO's service catalog.

Once the MNO has available the NESTs associated to the requested communication services (step 3), the Product Order Manager located in the *Business Support System (BSS)* has to map the NEST attributes with the slicing information models defined by the 3GPP. Specifically, the S/P-NEST attributes are translated into the service profile (step 4) [27]. The service profile is just an adaptation from the description language used in the GST. In turn, the *Network Slice Management Function (NSMF)* has to translate the attributes of the service profile into the requirements supported in each network segment. Focusing on the RAN, this procedure results in the definition of the RAN slice profile (step 5). The information gathered in the RAN slice profile will be used by the *RAN Network Slice Subnet Management Function (NSSMF)* to manage and orchestrate the RAN slices throughout their lifetimes. Within this management entity, the proposed RAN Slice Planner must execute all the procedures described in Section III-A. To that end, the RAN Slice Planner needs to take as input the parameters defined in the RAN slice profile. Table 1 describes those parameters considered in this work.

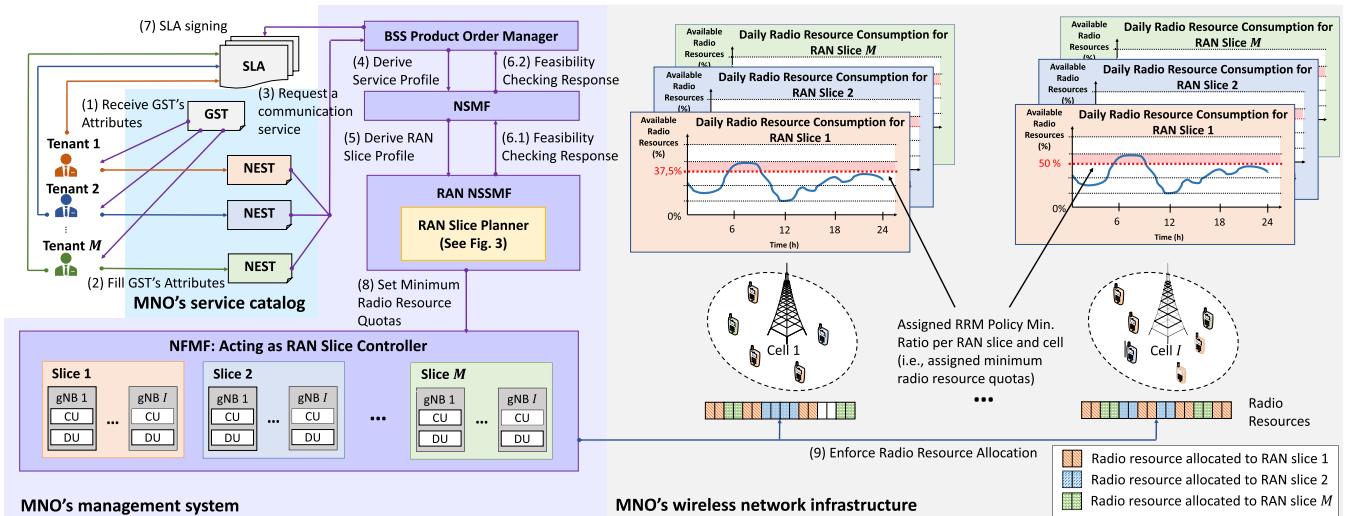


FIGURE 2. Integration of the RAN Slice Planner within the 3GPP RAN slice management framework.

TABLE 1. RAN slice profile's attributes considered as inputs for the proposed RAN Slice Planner.

RAN slice profile's attributes defined in [27]	Definition	Aspects considered by the proposed RAN Slice Planner
Service Area	This parameter specifies the area where the UEs can access a particular communication service. There are two ways of describing the coverage area: a) based on cell location or b) based on geographical partitioning.	Geographical partitioning is more reasonable because the MNO has not to expose tenants the cell location. The disadvantage is the MNO has to translate the geographical partitioning into the specific cells. In our work, the RAN Slice Planner performs this translation.
Downlink throughput per UE	This parameter defines the downlink data rate for a UE served by a specific network slice. Two types are defined: a) guaranteed downlink throughput and b) maximum downlink throughput.	In this work, we assume all the UEs served by a RAN slice consume a specific GBR for downlink traffic. Specifically, we consider these UEs generate sessions following a Poisson distribution. If a UE session cannot consume the GBR, it is rejected (i.e., blocked).
UE density	This parameter describes the maximum number of connected and/or accessible devices per unit area supported by the network slice.	The proposed RAN Slice Planner considers the UE spatial distribution instead of the average UE density. The reason is UE density could be different along the cells which comprise the entire coverage area. The average value is insufficient to describe this variability. To measure the accessibility, we also consider an upper bound for the UE blocking probability of a RAN slice in each cell. Using this parameter, the RAN Slice Planner can guarantee a percentage of accessible UE sessions for each RAN slice. We also assume this parameter is set up by the MNO and is the same for all the RAN slices.
Maximum Number of UEs	This parameter describes the maximum number of UEs that can be connected to a specific network slice simultaneously.	In the overall network, the MNO considers this parameter to estimate the busy hour. Later, the RAN Slice Planner limits the maximum number of UEs by imposing the upper bound for the UE blocking probability. This means that the maximum number of UEs will depend on (a) the radio channel conditions and (b) the radio resource quotas assigned for each RAN slice.
Service Availability (Service Request Success Rate)	The service availability represents the percentage value of the amount of time the end-to-end communication service is delivered according to a specified QoS, divided by the amount of time the system is expected to deliver the end-to-end service. One of the Key Performance Indicators (KPIs) to measure the service availability is the service request success rate, which represents the probability the request of a data session is successful.	A communication service is considered unavailable if it does not meet the pertinent QoS requirements. In the case of a GBR service, it is not available for each single UE if it cannot establish a data session with an average data rate equal to the GBR (i.e., the data session is blocked). This means that a lower UE blocking probability involves a higher service availability. Thus, the MNO must set the upper bound for the UE blocking probability in such a way that the service request success rate (i.e., the complementary probability of the UE blocking probability) defined in the SLA is met.

Focusing on the computation of the radio resource quotas, the RAN Slice Planner could consider different types of quotas in function of the policies imposed by the MNO. The 3GPP has standardized three policies denoted as Radio Resource Management (RRM) Policy Ratios [27], [34]:

- **RRM Policy Dedicated Ratio (optional policy):** It defines the dedicated radio resource quota for the associated RAN slice, i.e., its dedicated radio resources. These radio resources cannot be shared even if the associated RAN slice does not use them throughout its lifetime.

- **RRM Policy Minimum Ratio (mandatory policy):** It defines the minimum radio resource quota for the associated RAN slice, including prioritized radio resources and dedicated radio resources. Prioritized radio resources are those which are preferentially used by the associated RAN slice. When prioritized radio resources are not used by the associated RAN slice throughout its lifetime, other RAN slices could use them.
- **RRM Policy Maximum Ratio (mandatory policy):** It defines the maximum radio resource quota for the associated RAN slice, including shared radio resources, prioritized radio resources and dedicated radio resources. Shared radio resources are those which are shared among all RAN slices. This means the shared radio resources are not guaranteed for use by the associated RAN slice throughout its lifetime.

In this work, we focus on the RRM Policy Minimum Ratio. Specifically, the RAN Slice Planner translates the RAN slice profile's attributes defined in Table 1 for each RAN slice into the minimum radio resource quotas adopted in each cell. Then, the MNO proceed with the SLA signing (steps 6, 7). After that, the RAN NSSMF sends the computed radio resource quotas (step 8) to the Network Function Management Function (NFMF). Finally, the NFMF enforces the radio resource allocation performed in each cell during the operation of each RAN slice meets the bounds imposed by these quotas (step 9). This means each RAN slice will have available at least the amount of radio resources defined by these quotas if the traffic demand requires them.

In case the MNO cannot accommodate in a first attempt the requested RAN slices (i.e., at least a negative checking response is generated in Step 6), it may renegotiate the SLA with the tenants which requested the new RAN slices. In this scenario, the BSS Product Order Manager (a) must communicate the corresponding tenants that the requested requirements for their RAN slices cannot be satisfied and (b) may suggest them which specific requirements could be re-adjusted (e.g., a RAN slice with a lower maximum number of UEs). If the tenants accept the proposed re-adjustment, they need to re-set the corresponding GST's attributes. This means the steps 2-6 are repeated until all the RAN slices are accommodated into the RAN. Note that in this iterative procedure each tenant and/or the MNO may consider the SLA renegotiation is unfeasible for a specific RAN slice. In such a case, the MNO discards this RAN slice from the planning procedure.

IV. SYSTEM MODEL

In this work, we focus on the downlink operation of a 5G-New Radio (NR) multi-cell environment with several RAN slices. Each RAN slice provides a GBR service to their UEs, which dynamically request and release data sessions. In this scenario, the MNO must ensure the average rate for each data session must be above a specific value to provide the minimum quality of service that such RAN slice requires, e.g.,

an enhanced Mobile Broadband (eMBB) service providing video streaming requires 5 Mbps for full HD quality. For such reason, we assume all the admitted data sessions for single RAN slice have an average rate equal to the GBR specified by the tenant in the NEST, i.e., the attribute downlink throughput per UE described in Table 1. Furthermore, each cell supports Link Adaptation (LA) to allocate radio resources based on the channel quality, thus these cells consider the channel quality perceived by each UE to allocate them radio resources. Under this scenario, we first describe the network model. Then, we present the model for the radio resources. Next, we describe the channel model of a single cell. Finally, we define the characteristics of the offered traffic.

A. NETWORK MODEL

We consider a MNO owns a RAN infrastructure consisting of a set \mathcal{C} of 5G NR cells. Before the MNO initiates a planning period, we assume: (a) multiple tenants have requested in advance one or more communication services; and (b) there exist RAN slices which are currently running in the RAN infrastructure. Defining \mathcal{M} as the set of requested and activated RAN slices, the MNO will execute a RAN slice planning procedure with the aim of checking the feasibility of accommodating these RAN slices, each with specific GBR requirements over a certain subset $\mathcal{C}^m \subseteq \mathcal{C}$ of cells.

The traffic demand of each RAN slice is non-uniformly distributed over the considered RAN. Accordingly, the area of each cell has a different size to absorb the aggregated traffic demand from all the RAN slices with a maximum usage efficiency. In this work, we consider the cell location has already been established by the MNO. Specifically, we have adopted the algorithm proposed in [4] to determine the location and size of each cell. Under this scenario, a set \mathcal{U} of UEs exist, being (a) $\mathcal{U}^m \subseteq \mathcal{U}$ the subset of UEs served by the RAN slice m ; (b) $\mathcal{U}_i \subseteq \mathcal{U}$ the subset of UEs served by the cell $i \in \mathcal{C}$; and (c) $\mathcal{U}_i^m = \mathcal{U}^m \cap \mathcal{U}_i$ the intersection of both subsets.

B. RADIO RESOURCE MODEL

We assume Orthogonal Frequency-Division Multiple Access (OFDMA) as accessing scheme. Focusing on a single cell $i \in \mathcal{C}$, it supports a total bandwidth W_i . In turn, this bandwidth is divided into N_i OFDM sub-carriers, which are grouped in groups of $N_{SC} = 12$ sub-carriers. Each group defines a Resource Block (RB), which is the smallest unit of resources that can be allocated to a UE. The number of available RBs on average during a time slot is given by Eq. (1). Since a 5G NR cell supports scalable numerologies ($\mu = 0, 1, \dots, 4$), the subcarrier spacing is computed as $\Delta_f = 2^\mu \cdot 15$ KHz. The parameter OH denotes the overhead factor due to control plane data [35].

$$N_{RB,i}^{slot} = \left\lfloor \frac{W_i}{N_{SC} \Delta_f} (1 - OH) \right\rfloor. \quad (1)$$

In a single carrier, the number of RBs could range from 11 to 273 units [36], [37]. This means $N_{RB,i}^{slot}$ could be high if the cell i employs a small numerology and a large

bandwidth. Then, from the perspective of radio resource allocation in RAN slicing, it becomes advantageous to reduce the management complexity by grouping the RBs into resource chunks, which are allocated to the RAN slices as indivisible units [7]. This can be done through the concepts of Bandwidth Part (BWP) and Resource Block Group (RBG) defined in [38] and [39], respectively. A BWP is a continuous set of RBs for a given numerology. A RBG is a collection of consecutive RBs within a given BWP that can be allocated to a specific UE. The size of the RBG, herein denoted as R_{size} , can be used for establishing the minimum allocation unit size. Increasing R_{size} may serve to reduce the signaling overhead at the expense of a loss of flexibility, which could be critical when the number of RAN slices to be planned is large. Under these considerations, we denote (a) \mathcal{R}_i as the set of RBGs in cell i , (b) $\mathcal{R}_i^m \subseteq \mathcal{R}_i$ as the subset of RBGs allocated to the slice m in cell i ; and (c) $\mathcal{R}_i^u \subseteq \mathcal{R}_i^m$ as the subset of RBGs allocated to a UE u which is served by the RAN slice m in the cell i . Finally, we can compute the available RBGs on average during a time slot in the cell i as $R_i^{slot} = \lfloor N_{RB,i}^{slot} / R_{size} \rfloor$. Note that the sum of RBGs allocated for each RAN slice, i.e., $R_{i,m}^{slot}$, must be less or equal than R_i^{slot} .

C. CHANNEL MODEL

To measure the channel quality within each cell, we consider the average Signal-to-Interference-plus-Noise Ratio (SINR). Specifically, we define in Eq. (2) the average SINR $\gamma_{u,r}$ measured by the UE $u \in \mathcal{U}$ in the RBG $r \in \mathcal{R}_i^m$. The parameter P_i^{RX} denotes the received power. This power results from the transmitted power minus the attenuation suffered by the shadow fading and the path loss. The fast fading is not modeled since the average SINR is measured over a large time scale. Note that we assume the same transmitted power for all the RBGs. The parameter $\Gamma(u)$ is a function that returns the cell $i \in \mathcal{C}^m$ which the UE u served by the RAN slice m is attached to. This cell is the one from which this UE receives the strongest average SINR. Finally, the parameter $I_{u,r,i}$ denotes the interference suffered by the UE u in the RBG r , and P_N is the noise power measured in one RBG.

$$\gamma_{u,r} = \frac{P_i^{RX}}{I_{u,r,i} + P_N} \quad | i = \Gamma(u). \quad (2)$$

The interference $I_{u,r,i}$ is provided in Eq. (3). This parameter is split into two summations, each gathering the intra-slice and inter-slice interference terms, respectively. An interference term j is intra-slice when the RBG r from neighbor cell j is allocated to the same RAN slice m which serves the user u in the cell i . An interference term j is inter-slice when the RBG r from neighbor cell j is allocated to a RAN slice n different from the slice m . To identify these terms, we use the binary variable $\delta_{u,r,j}$. It takes the value 1 when the interference term is intra-slice and the value 0 otherwise.

$$I_{u,r,i} = \sum_{j \in \mathcal{C} \setminus \{i\}} L_{j,r} \alpha_{j,r} P_j^{RX} \delta_{u,r,j}$$

$$+ \sum_{j \in \mathcal{C} \setminus \{i\}} L_{j,r} \alpha_{j,r} P_j^{RX} (1 - \delta_{u,r,j}). \quad (3)$$

The parameter $\alpha_{j,r}$ is also a binary variable that takes the value 1 when the RBG r is allocated to the neighbor cell j and the value 0 otherwise. The value for $\alpha_{j,r}$ will depend on the radio resource allocation performed by the RAN Slice Planner in each neighbor cell. Finally, $L_{j,r}$ denotes the cell load factor, which is given by Eq. (4). In this equation, $\beta(j, r)$ is a function that indicates the RAN slice m for which the RBG r from cell j has been allocated. The parameter th_m denotes the average data rate consumed by a UE data session belonging to the RAN slice m . In this work, we assume all the data sessions for a RAN slice require an average data rate equal to the GBR specified in the SLA. Note that the number of UEs served by the RAN slice m in cell j is given by $|\mathcal{U}_j^m|$. The parameter $SE_{u,r}$ is the average data rate per bandwidth unit (i.e., spectral efficiency) for the UE u in the RBG r . Unlike our previous work [7], we consider that only the RBGs allocated to a specific RAN slice can be scheduled to the UEs attached to this RAN slice. This means each RAN slice m produces a different load in a specific cell in function of its GBR requirements and the number of allocated RBGs.

$$\hat{L}_{j,r} = \frac{|\mathcal{U}_j^m| th_m}{N_{SC} \Delta_f \sum_{u \in \mathcal{U}_j^m} \sum_{r \in \mathcal{R}^u} SE_{u,r}} \quad | m = \beta(j, r). \quad (4a)$$

$$L_{j,r} = \min(\hat{L}_{j,r}, 1). \quad (4b)$$

The average spectral efficiency $SE_{u,r}$ is recursively derived from $\gamma_{u,r}$ as Eq. (5) shows. The parameter SE_{max} denotes the maximum achievable spectral efficiency with LA, γ_{min} and γ_{max} the minimum and maximum average SINR values, respectively. Finally, σ is an attenuation factor due to implementation losses [40].

$$SE_{u,r} = \begin{cases} 0, & \gamma_{u,r} < \gamma_{min}; \\ \sigma \cdot \log_2(1 + \gamma_{u,r}), & \gamma_{min} \leq \gamma_{u,r} < \gamma_{max}; \\ SE_{max}, & \gamma_{u,r} > \gamma_{max}; \end{cases} \quad (5)$$

D. TRAFFIC MODEL

To model the traffic demands of each individual RAN slice, we consider the statistical distributions and the average values for the arrival rate of UE sessions and the session duration. These average values correspond to the ones which could be measured during the busy hour. We assume the MNO has previously estimated them (see steps 1-2 in Fig. 1).

Regarding the arrival rate of UE sessions for RAN slice m , we assume an average of λ_m requests per unit time following a Poisson distribution. It is well known that in many cases, the sum of a large number of independent stationary renewal processes (i.e., in our scenario, each individual UE generating data sessions), each with an arbitrary distribution of renewal time, will tend to a Poisson process [41]. Since a Poisson process can be split into independent processes [42], we can also express the average arrival rate for each cell as $\lambda_{i,m} =$

$\omega_{i,m}\lambda_m$. The variable $\omega_{i,m}$ denotes the probability a UE $u \in \mathcal{U}^m$ is served by the cell i . This probability will depend on:

- (a)
 - 1) The UE density distribution (see Table 1) for the RAN slice m in the entire RAN, i.e., the probability an arbitrary UE served by this RAN slice is located in a specific position in the geographical area covered by the RAN. We assume each RAN slice presents a specific UE spatial distribution.
 - 2) The average SINR perceived by each UE from each cell. Specifically, we consider each UE is served by the cell from which it perceives the strongest SINR.

With respect to the session duration $t_{u,m}^{ses}$ for each UE u served by the RAN slice m , we assume a random variable extracted from an arbitrary distribution. This means we could consider a different distribution for each RAN slice. Additionally, we define $\mu_m = 1/E[t_{u,m}^{ses}]$ as the average rate for releasing UE sessions per unit time of the RAN slice m .

Defined $\lambda_{i,m}$ and μ_m , we compute the average offered traffic intensity for the RAN slice m in each cell i as $\rho_{i,m} = \lambda_{i,m}/\mu_m$. Furthermore, the total average offered traffic intensity for this RAN slice is also computed as $\rho_m = \sum_{i \in \mathcal{C}} \rho_{i,m}$.

Finally, to model the probability of blocking the data session of a UE $u \in \mathcal{U}_i^m$ served by the RAN slice m in cell i , i.e., $B_{i,m}$, we use the analytical model which we proposed in [43]. In this model, we consider a multi-dimensional Erlang-B system where each dimension represents a specific range of values for the average SINR which a UE could perceive in the cell. To compute the UE blocking probability, this model considers as inputs: (a)

- 1) A discrete set of values for $\gamma_{u,r}$, each one associated to a dimension of the multi-dimensional Erlang-B system. Specifically, each value is the average within the range of values for the average SINR defined in the corresponding dimension.
- 2) The probability that a UE session perceives an average SINR within the range of values defined for each dimension.
- 3) The amount of radio resources \mathcal{R}_i^m which are guaranteed for the RAN slice in the cell, i.e., the radio resource quota.

For more detailed information about the model for the UE blocking probability, we recommend the reader to see [43].

V. RADIO RESOURCE PLANNING BASED ON ORDINAL POTENTIAL GAMES

A. PROBLEM FORMULATION

In this work we analyze the radio resource planning for RAN slices providing GBR services. Specifically, we formulate the planning process as Eq. (6a) shows. The goal of our RAN slice planning is to minimize the average UE blocking probability $\bar{B}_{m'}$ of the RAN slice m' which has the highest value for this parameter. For each RAN slice m , the average UE blocking probability can be computed as $\bar{B}_m = \sum_{i \in \mathcal{C}^m} \omega_{i,m} B_{i,m}$. Note that the UE blocking probability

B_i^m for the RAN slice m in cell i depends on (a) the radio resource allocation for this RAN slice in this cell, i.e., \mathcal{R}_i^m and (b) the radio resource allocation for all the RAN slices in the neighbor cells. The constraints given in Eq. (6b) enforce the UE blocking probability $B_{i,m}$ for each RAN slice m in each cell i is below the upper bound B^{th} . We assume this bound on the UE blocking probability is established by the MNO before receiving any RAN slice request and it is the same for all the RAN slices.

$$\min_{\mathcal{R}_i^m} \max (\bar{B}_1, \bar{B}_2, \dots, \bar{B}_m, \dots, \bar{B}_M) \quad \forall i \in \mathcal{C}; \quad \forall m \in \mathcal{M}. \quad (6a)$$

$$\text{s.t. } B_{i,m} \leq B^{th}. \quad (6b)$$

The objective function defined in Eq. (6a) is a non-convex function and thus with at least NP-hard complexity. This fact is mainly due to the inter-cell interference. For instance, the higher the number of RBs are allocated for the RAN slice m in the cell i , the lower the UE blocking is. However, the inter-cell interference increases in each neighbor cell $j \in \mathcal{C} \setminus \{i\}$, meaning the UE blocking probabilities $B_{j,m}$ for all the RAN slices in the neighbor cells increase, and thus the objective function may also increase. This involves the existence of multiple local minima in the considered search space. Solving the formulated problem can be seen as a combinatorial optimization, i.e., searching the best combination of allocated radio resources $|\mathcal{R}_i^m|$ for each RAN slice $m \in \mathcal{M}$ in each cell $i \in \mathcal{C}$ which minimizes the cost function. Performing an exhaustive search to find the optimal solution is not computationally tractable, especially when the number of cells $|\mathcal{C}|$, RBs per cell $|\mathcal{R}_i|$ and RAN slices $|\mathcal{M}|$ are considerably high. As an alternative, searching a local optimum is a better option. By using game theory to model the formulated problem, we can find a local optimum by determining a NE solution. In this work, we model our problem as multiple ordinal potential games and demonstrate the existence of a NE solution.

On the one hand, since the neighbor cells may cause interference on a given cell, the MNO must consider each cell as a selfish entity which tries to meet the performance requirements of the RAN slices that it serves. In our proposal we consider multiple potential games where the selfish entities are the cells instead of the tuple defined by one cell and one RAN slice. Considering a higher number of players (e.g., a player per cell and per RAN slice) would involve higher complexity. For such a reason, our approach simplifies the game because less players are considered.

On the other hand, the RAN slice planning must be executed in the RAN NSSMF,² which is a logically centralized entity as Fig. 2 describes. For this reason, we consider the

²Note that once the RAN slice planning procedure ends and the requested RAN slices are activated, the RAN NSSMF enforces the computed 3GPP policy ratios to each RAN slice in each cell by means of the NFMMF (see step 8 in Fig. 2).

proposed multiple potential games are executed in a centralized way by the RAN NSSMF. To that end, all the players must have the same utility function, i.e., in game theory, it is a mathematical function which each player aims to unilaterally optimize. Although the common approach in game theory is to execute a game in a distributed way, i.e., by considering each player has a specific utility function, there exist games in the literature where all the players share a common utility function. These games are known as identical-interest games and perfect coordination games [44]. Our proposed potential games are equivalent to them.

B. PROPOSED POTENTIAL GAMES

In game theory, a game is defined as $\mathcal{G} = [\mathcal{C}, \{S_i\}_{i \in \mathcal{C}}, \{\Phi_i\}_{i \in \mathcal{C}}]$ where \mathcal{C} is the set of players participating in the game, S_i is the strategy selected by player i , and $\Phi_i : S \rightarrow \mathbb{R}$ is the utility function of that player, with S the strategy profile of the game (i.e., the set of strategies selected by all the players). If we refer to a single player, i.e., the i^{th} player, then S can be rewritten as $S = (S_i, S_{-i})$, where S_{-i} denotes the joint strategy adopted by player i 's opponents. In a game \mathcal{G} , each player will choose selfishly a new strategy T_i in its turn with the aim of improving its utility function considering the current strategies of the other players. A game is an ordinal potential game if and only if a potential function $F(S)$ exists such that Eq. (7) is met, where $\text{sgn}[\cdot]$ denotes the signum function [45].

$$\begin{aligned} \text{sgn}[\Phi_i(T_i, S_{-i}) - \Phi_i(S_i, S_{-i})] \\ = \text{sgn}[F(T_i, S_{-i}) - F(S_i, S_{-i})] \quad \forall i \in \mathcal{C}. \end{aligned} \quad (7)$$

In our game, the set of players \mathcal{C} are the cells where the requested RAN slices will be deployed and the existing RAN slices are running. For every i^{th} cell, a strategy S_i consists of a specific RBG allocation for all the RAN slices which require the coverage of this cell. In turn, the utility function for each i^{th} cell Φ_i is given by Eq. (8). As previously stated, the utility function is the same for all the players, our game could be seen as identical-interest game or perfect coordination game [44].

$$\Phi_i = (\max(\bar{B}_1, \bar{B}_2, \dots, \bar{B}_m, \dots, \bar{B}_M))^{-1} \quad \forall m \in \mathcal{M}. \quad (8)$$

The potential function $F(S)$ is defined by Eq. (9). Since the utility function of each cell i is equal to the potential function, i.e., $\Phi_i(S_i, S_{-i}) = F(S_i, S_{-i}) \quad \forall i \in \mathcal{C}$, it is straightforward that Eq. (7) is always met. Thus, an unconstrained game including the potential function $F(S)$ and utility functions $\Phi_i \quad \forall i \in \mathcal{C}$ is an ordinal potential game. Consequently, the proposed game always reaches a NE solution. Note that game theory states that if a game is a potential game, it always has a NE solution [45].

$$F(S) = (\max(\bar{B}_1, \bar{B}_2, \dots, \bar{B}_m, \dots, \bar{B}_M))^{-1} \quad \forall m \in \mathcal{M}. \quad (9)$$

Defined the utility functions and the potential function, we formulate our constrained game \mathcal{G} as Eq. (10) shows. The

goal of this game is to determine the set of strategies S , i.e., the RBG allocation for each RAN slice in each cell, which maximize the potential function.

$$(\mathcal{G}) : \forall i \in \mathcal{C} \max_{S_i \in S^i} \Phi_i(S_i, S_{-i}) \text{ s.t. } g_{i,m}(S_i, S_{-i}) \leq 0. \quad (10)$$

We also assume there are $|\mathcal{C}| \cdot |\mathcal{M}|$ inequalities constrains in the form of $g_{i,m}(S) \leq 0$. Specifically, these constrains are expressed by Eq. (11). In [45], the authors proof that a constrained game is an ordinal potential game only if the equivalent game without constraints is also an ordinal potential game. This means that the proposed constrained game \mathcal{G} is an ordinal potential game.

$$g_{i,m}(S) = B_{i,m} - B_m^{\text{th}} \quad \forall m \in \mathcal{M}, \quad \forall i \in \mathcal{C}. \quad (11)$$

To perform the radio resource planning, the proposed RAN Slice Planner could follow two approaches: one-game-all, and consecutive games.

In the one-game-all approach, the RAN Slice Planner executes the game \mathcal{G} with $M' = |\mathcal{M}|$ RAN slices. In this game, the starting point is the allocation of one RBG for each RAN slice in the cells where they require coverage.

In the consecutive games approach, the RAN Slice Planner executes $|\mathcal{M}|$ consecutive games as the one formulated in Eq. (10). In each m^{th} game, only $M' = m$ RAN slices participate. Focusing on the first game, i.e., $M' = 1$, the RAN Slice Planner performs the RBG allocation for one RAN slice. In this game, the starting point is the allocation of one RBG in each cell where this RAN slice requires coverage. When the RAN Slice Planner executes the first game, it considers the derived RBG allocation as the starting point of the next game, where $M' = 2$ RAN slices participate. The RAN Slice Planner repeats this procedure until it executes the $|\mathcal{M}|^{\text{th}}$ game.

As we demonstrate in Section VII-D, the proposed game tends to equal the average UE blocking probabilities of all the RAN slices. This means that selecting a starting point of the game where the average UE blocking probabilities of all the RAN slices are closer could involve reaching a NE solution where all the average UE blocking probabilities are equaled and minimized, but the constraints given by Eq. (11) are not met. This scenario is frequent when the RAN Slice Planner follows the one-game-all approach. To avoid this issue, we consider the RAN Slice Planner follows the consecutive game approach.

VI. PLANNING METHOD BASED ON BETTER RESPONSE DYNAMICS

In Fig. 3, we illustrate a block diagram which summarizes the behavior of the proposed RAN Slice Planner. In a planning period, this mathematical framework executes $|\mathcal{M}|$ consecutive ordinal potential games. Focusing on a specific game \mathcal{G} with $M' \leq |\mathcal{M}|$ RAN slices,³ the RAN Slice Planner selects the next cell player i and determines the strategy T_i

³The order in which the RAN slices enter into a game is out of the scope.

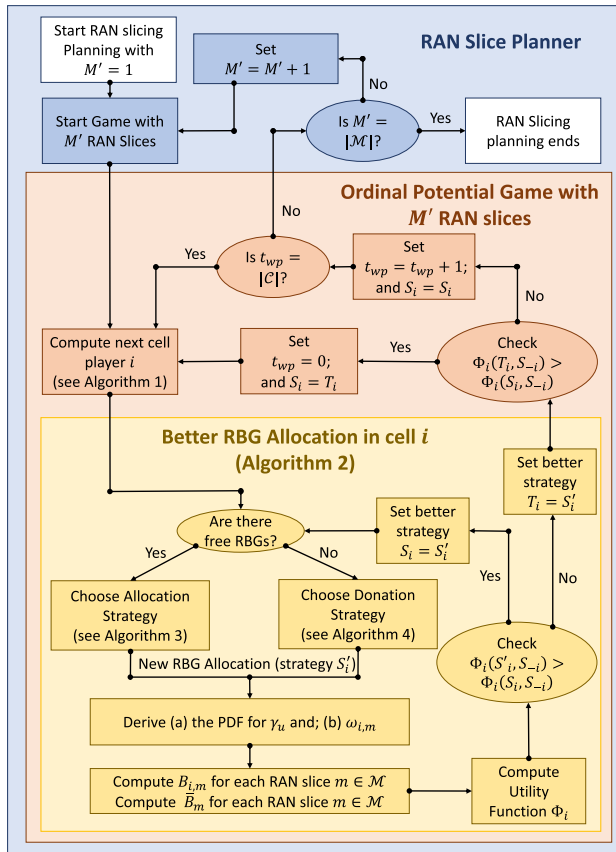


FIGURE 3. High-level view of the methods implemented by the RAN Slice Planner to perform the planning of $|\mathcal{M}|$ RAN slices.

which provides the better RBG allocation for each RAN slice in such cell. The method to determine such allocation is based on better response dynamics, i.e., the players proceed toward a NE solution via a local search method. Then, if the utility function Φ_i of this cell improves with respect to the previous strategy S_i , i.e., $\Phi_i(T_i, S_{-i}) > \Phi_i(S_i, S_{-i})$, the RAN Slice Planner considers T_i as the new strategy S_i in this cell and computes the next cell player. If the utility function Φ_i does not improve with respect to the previous strategy S_i , it remains as the better strategy for this cell. In such case, the RAN Slice Planner also increases by one a counter t_{wp} that records the cell players which cannot improve their utility functions. The game \mathcal{G} will end when none of the cell players can improve its utility function, i.e., $t_{wp} = |\mathcal{C}|$. If this happens, the RAN Slice Planner will execute more games until the number of executed games is $|\mathcal{M}|$. At this point, the RAN Slice Planner will have determined the minimum radio resource quotas for each RAN slice in each cell by considering the strategies $S_i \forall i \in \mathcal{C}$ derived in the $|\mathcal{M}|$ th game.

If the computed radio resource quotas satisfy the performance requirements of all the RAN slices (see Eq. 6b), the RAN slice planning in this planning window will have ended. Otherwise, a renegotiation (and/or network extension) phase

Algorithm 1 Computing the Next Cell Player i'

- 1 Inputs: $\bar{B}_m, B_{i,m}$, and $\omega_{i,m} \forall m \in \mathcal{M} \forall i \in \mathcal{C}$;
- 2 Determine $m' = \arg \max [(\bar{B}_1, \dots, \bar{B}_{|\mathcal{M}|})]$;
- 3 Compute $i' = \arg \max [(\omega_{1,m'} B_{1,m'}, \dots, \omega_{|\mathcal{C}|,m'} B_{|\mathcal{C}|,m'})]$

starts. At this point, the MNO and the corresponding tenants renegotiate the SLA by e.g., reducing the required GBR (and/or extending the network by e.g., adding new carriers in each cell). After that, the procedure illustrated in Fig. 3 is re-executed until either all the requested RAN slices can be accommodated in the RAN or, conversely, some of them are discarded by the MNO (e.g. considering economic aspects).

In the following subsections, we provide details about the method used by the RAN Slice Planner to define the order in which each cell selects its better RBG allocation as well as the method to determine such allocation.

A. METHOD TO DECIDE THE NEXT CELL PLAYER

In our game, we aim to maximize the potential function $F(S)$ using the minimum number of iterations, where each iteration corresponds to the set of actions taken by a cell player to determine its better RBG allocation. When better response dynamics is used for computing the NE solution, the computational time to reach this solution strongly depends on the order in which players are chosen to perform their actions. Better response dynamics leaves unspecified the rules to define this order [46].

To minimize the required number of iterations for reaching the NE solution, the RAN Slice Planner executes Algorithm 1, which decides the next cell player. First, this algorithm determines the RAN slice m' which provides the maximum average UE blocking probability. Then, considering the weighted UE blocking probability for the selected RAN slice m' in each cell (i.e., $\omega_{i,m'} B_{i,m'}$), the algorithm selects as the next player i' the cell where the weighted UE blocking probability is maximum. Using the proposed algorithm, the RAN Slice Planner selects the cell where the RAN slice which provides the value for the potential function, see Eq. (9), has the worst weighted UE blocking probability. In this way, the RAN Slice Planner can reallocate RBGs in such cell with the goal of maximizing the potential function much faster.

B. BETTER RBG ALLOCATION IN THE CELL PLAYER

Algorithm 2 provides the steps performed by the RAN Slice Planner to select the better RBG allocation (i.e., strategy T_i) in the cell player i . These steps are also depicted in Fig. 3. First, the RAN Slice Planner checks if there are free RBGs in the cell i , i.e., those RBGs which have not been allocated for any RAN slice. If so, one free RBG will be allocated to RAN slice m' (i.e., the RAN slice derived by Algorithm 1). Algorithm 3 details how the RAN Slice Planner selects this RBG (see Section VI-C). If there are not free RBGs, the only

Algorithm 2 Computing the Better RBG Allocation, i.e., Strategy T_i , for Cell Player i

```

1 Initialization: RBG allocation for each RAN slice in
  cell  $i$ , i.e.,  $S_i$ ;
2 found_better_strategy = false;
3 while found_better_strategy == false do
4   if free_RBGs == true then
5     Allocate one RBG to RAN slice  $m'$  (see
     Algorithm 3)  $\rightarrow$  New strategy  $S'_i$ ;
6   else
7     Compute  $m'' = \arg \min(\omega_{i,m} B_{i,m})$ 
      $\forall m \in \mathcal{M} \setminus \{m'\}$ ;
8     Donate one RBG from RAN slice  $m''$  to RAN
     slice  $m'$  (see Algorithm 4)  $\rightarrow$  New strategy
      $S'_i$ ;
9   end
10  From  $S = (S'_i, S_{-i})$ , derive  $f_{PDF}(\bar{\gamma}_u)$  for each
    pair of RAN slice an cell.  $\omega_{i,m}$  is also derived
     $\forall i \in \mathcal{C}$  and  $\forall m \in \mathcal{M}$ ;
11  Compute  $B_{i,m} \forall i \in \mathcal{C}, \forall m \in \mathcal{M}$ ;
12  Compute  $\bar{B}_m \forall m \in \mathcal{M}$ ;
13  Compute  $\Phi_i(S'_i, S_{-i})$ ;
14  if  $\Phi_i(S'_i, S_{-i}) > \Phi_i(S_i, S_{-i})$  then
15     $S_i = S'_i$ ;
16  else
17     $T_i = S_i$ ;
18    found_better_strategy = true;
19  end
20 end
21 return:  $T_i$ 

```

way to reduce the average UE blocking probability for RAN slice m' is to allocate it one RBG from another RAN slice. To that end, the RAN Slice Planner determines the RAN slice m'' which has the lowest weighted UE blocking probability in cell i . Then, one RBG is donated from RAN slice m'' to RAN slice m' . Algorithm 4 details how the RAN Slice Planner determines the donated RBG (see Section VI-D).

After the RAN Slice Planner uses Algorithm 3 or Algorithm 4, it derives a new strategy S'_i resulted from the RBG reallocation in cell i . Based on that, the RAN Slice Planner computes $|\mathcal{C}| \cdot |\mathcal{M}|$ Probability Density Functions (PDFs) of the average SINR experienced by an arbitrary UE, i.e., $f_{PDF}(\bar{\gamma}_u)$, one per each pair of RAN slice and cell. During this procedure, the probability that an arbitrary UE is attached to a specific cell $\omega_{i,m}$ is also recomputed. The proposed algorithm uses the strongest SINR as the criteria to attach each UE to a specific cell.

After deriving these PDFs, the RAN Slice Planner computes the UE blocking probability for each RAN slice in every cell, i.e., $B_{i,m}$ by using the model we proposed in [43]. Then, the RAN Slice Planner computes the mean UE blocking probability for each RAN slice, and thus it derives the new value for the utility function $\Phi_i(S'_i, S_{-i})$ of the cell i . Next, the RAN

Algorithm 3 Allocation of One RBG r' to the RAN Slice m'

```

1 Initialization:  $dist_{cells}(i') = \infty \forall i' \in \mathcal{C} \setminus \{i\}$ ;
2 for  $r \in \mathcal{R}_i^{free}$  do
3   for  $i' \in \mathcal{C} \setminus \{i\}$  do
4     if  $r \notin \mathcal{R}_{i'}^{free}$  then
5       Compute  $dist_{cells}(i') = ED(i, i')$ ;
6     end
7   end
8   Compute  $dist_{RBG}(r) = \min(dist_{cells}(i'))$ ;
9 end
10 Compute  $r' = \arg \max(dist_{RBG}(r))$ ;
11 return:  $r'$ 

```

Slice Planner compares the new value of the utility function with respect to the previous one, calculated from the old RBG allocation S_i . If the utility function improves, then the new RBG allocation is considered as the valid strategy (i.e., $S_i = S'_i$). In this case, steps from 4 to 19 are repeated until the RAN Slice Planner cannot improve the utility function. When this happens, the RAN Slice Planner ends the execution of Algorithm 2 and the better RBG allocation is the one derived in the previous iteration, i.e., T_i .

In the following subsections, we provide details about the steps performed by Algorithms 3 and 4 to reallocate the RBGs to a cell player.

C. RBG ALLOCATION

To allocate one RBG r' to the RAN slice m' , the RAN Slice Planner executes the steps described in Algorithm 3. First, the RAN Slice Planner initializes to infinity the vector $dist_{cells}$. For each available RBG in the cell, i.e., $r \in \mathcal{R}_i^{free}$, the RAN Slice Planner checks if this RBG has been allocated in the neighbor cells. If so, $dist_{cells}$ stores the euclidean distance, given by the function $ED(\cdot)$, between the cell i and the neighbor cell i' . When this task is performed for all the neighbor cells, the RAN Slice Planner selects the minimum distance gathered in $dist_{cells}$. The goal is to determine the closest neighbor cell which interferes RBG r more strongly. Considering these interference levels and repeating this procedure for all the free RBGs, the RAN Slice Planner determines the RBG r' which suffers less interference.

D. RBG DONATION

To donate one RBG r' from the RAN slice m'' to m' , the RAN Slice Planner executes the steps described in Algorithm 4. First the RAN Slice Planner initializes to infinity the vector $dist_{cells}$. For each available RBG, the RAN Slice Planner checks if this RBG has been allocated in the neighbor cells. At this point, the behavior of the proposed algorithm is equal to Algorithm 3. The reason is this algorithm aims to donate the RBG r' which interfere less with the neighbors of the cell i . In this way, if the RAN slice m' would induce a higher cell

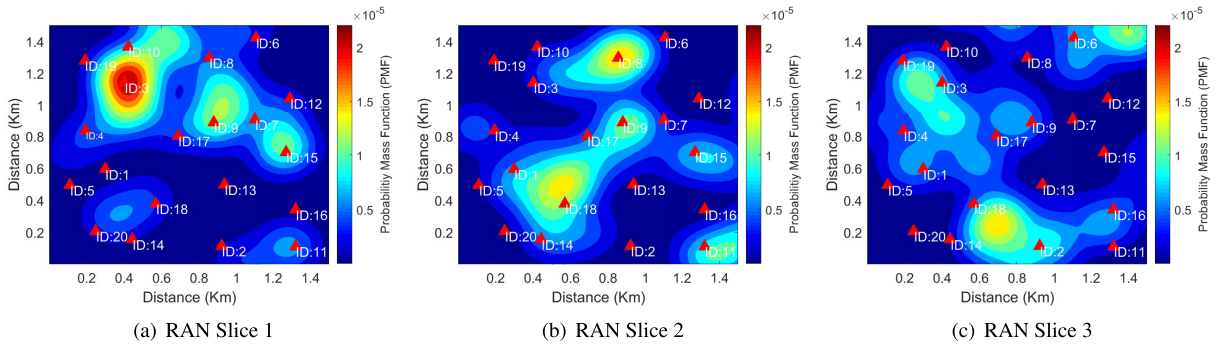


FIGURE 4. Probability Mass Function (PMF) of the UE location for each RAN slice.

Algorithm 4 Donation of One RBG r' From RAN Slice m'' to RAN Slice m'

```

1 Initialization:  $dist_{cells}(i') = \infty \forall i' \in \mathcal{C} \setminus \{i\}$ ;
2 for  $r \in \mathcal{R}_i^{m''}$  do
3   for  $i' \in \mathcal{C} \setminus \{i\}$  do
4     if  $r \notin \mathcal{R}_{i'}^{free}$  then
5       Compute  $dist_{cells}(i') = ED(i, i')$ ;
6     end
7   end
8   Compute  $dist_{RBG}(r) = \min(dist_{cells}(i'))$ ;
9 end
10 Compute  $r' = \arg \max(dist_{RBG}(r))$ ;
11 return:  $r'$ 

```

load in the RBG r' in comparison with the current cell load induced by the RAN slice m'' , see Eq. (4), the interference term induced in RBG r' would be minimum.

VII. NUMERICAL RESULTS AND DISCUSSIONS

In this section, we evaluate the performance of the proposed RAN Slice Planner. Specifically, since there are not solutions in the literature which address the planning of RAN slices with requirements on both the GBR and the UE blocking probability, we compare our proposal with two reference solutions. The reference solution 1 computes the minimum radio resource quota for a RAN slice m in a cell i as $R_{i,m}^{slot} = N_{RB,i}^{slot}/|\mathcal{M}|$, i.e., the radio resources are equally distributed between the RAN slices. The reference solution 2 computes the minimum radio resource quota as $R_{i,m}^{slot} = \left\lfloor \left(\rho_{i,m} / \sum_{m' \in \mathcal{M}} \rho_{i,m'} \right) N_{RB,i}^{slot} \right\rfloor$, i.e., the radio resources are distributed in proportion to the average offered traffic intensity of each RAN slice in such cell. For both reference solutions, we assume the specific RBGs that provide the given quotas are randomly allocated. In addition to the performance analysis, we also evaluate the renegotiation capability of the proposed solution.

A. EXPERIMENTAL SETUP

We consider a RAN infrastructure which comprises a set of $|\mathcal{C}| = 20$ cells deployed over an urban area of 1.5 Km x

1.5 Km. We also assume the traffic demand for each RAN slice is non-uniformly distributed over the considered area. In Fig. 4, we show the traffic demand distribution of some of the considered RAN slices. The triangles represent the location of the deployed access nodes and the colored surface indicates the Probability Mass Function (PMF) for the location where a specific RAN slice may serve a UE. To characterize the channel conditions of a UE served by a specific RAN slice, we use a snapshot-based model [7]. Each snapshot represents a random realization of the demand distribution for a RAN slice, i.e. varying the positions of the served UEs according to the PMFs shown in Fig. 4. The different realizations of the same traffic probability distribution ensure reliable statistical significance analysis. Specifically, these realizations allow us to estimate the spatial distribution of the average SINR and thus, compute the probability $\omega_{i,m}$ that an arbitrary UE belonging to the RAN slice $m \in \mathcal{M}$ is served by the cell $i \in \mathcal{C}$. With respect to the data sessions, we consider all the UEs of all the RAN slices will generate sessions following a Poisson distribution. Concerning the UE session duration, we consider each RAN slice will present one of the following distributions: exponential, uniform, or a constant duration. Finally, Table 2 summarizes the parameters used for the simulations.

All the experiments have been carried out on a computer with 16 GB RAM and an Intel core i7-4790 CPU @ 3.60 GHz.

B. CONVERGENCE ANALYSIS

The first experiment provides the computational complexity analysis of the proposed RAN Slice Planner. In this experiment, we assume the RAN Slice Planner must plan the deployment of three requested RAN slices with specific average offered traffic intensities, i.e., ρ_m . Specifically, we consider $\rho_1 = \rho_3 = \rho_0$, whereas ρ_2 could take different values from $0.25\rho_0$ to $4\rho_0$. To ease the comprehensibility of the proposed algorithms, we assume in this experiment there are not running RAN slices in the considered RAN.

In Fig. 5, we depict the evolution of the average UE blocking probability \bar{B}_m for each RAN slice when the RAN Slice Planner executes the multiple ordinal potential games. In this specific realization, we assume $\rho_2 = 2\rho_0$. When the game

TABLE 2. Simulation parameters.

Parameter	Configuration
Cellular Environment	Urban, 1.5 Km x 1.5 Km
Number of Cells $ \mathcal{C} $	20
Carrier frequency	2.14 GHz (i.e., within band n1 [36])
5G Numerology μ	0
Number of available RBs in a cell $N_{RB,i}^{slot}$ (same for all the cells)	106 RBs
RBG size R_{size}	4 RBs
Propagation (path loss, shadowing)	Umi model [47]
Cell antenna directivity	Omni-directional
Cell antenna height	6 m
UE antenna height	1.5 m
UE thermal noise	-174 dBm/Hz
UE noise figure	9 dB
UE minimum SINR γ_{min}	-10 dB [40]
UE maximum SINR γ_{max}	30 dB [40]
Attenuation factor σ	0.6
Maximum spectral efficiency SE_{max}	7.4063 bps/Hz
UE Downlink (DL) data rate per RAN slice th_m (same for all the RAN slices)	0.8 Mbps
Upper bound for the UE blocking probability B^{th}	1%
UE blocking probability model for each pair RAN slice - cell	See [45]
Number of RAN slices	From 3 to 6
Reference average offered traffic intensity ρ_0	2
Average offered traffic intensity per RAN slice ρ_m	From 0.25 to 4

$M' = 1$ starts, only the RAN slice $m = 1$ participates. In this game, the RAN Slice Planner iteratively adds radio resources in each cell for this RAN slice until a NE solution is reached. In the game $M' = 2$, the RAN Slice Planner first adds the remaining free RBGs (if available after finishing the previous game) and then it donates RBGs from the RAN slice $m = 1$ to the RAN slice $m = 2$. The aim of these procedures is to minimize the average UE blocking probability of the RAN slice which presents the highest value for this parameter. We observe how the average UE blocking probabilities of these RAN slices tend to be equal in the first iterations of this game (i.e., iteration 850 approx.). Then, the RAN Slice Planner slightly reduces these average UE blocking probabilities until reaching the NE solution (i.e., iteration 950 aprox.). Finally, the periodical peaks in the last iterations correspond to the situation where the cells cannot improve their utility functions. In the last game, i.e., $M' = 3$, the RAN Slice Planner acts in the same way as the previous game with the difference that RAN slices $m = 1$ and $m = 2$ donates radio resources to the new RAN slice.

With respect to the number of iterations performed by the proposed RAN Slice Planner, it is conditioned to the number of considered cells and RBGs per cell as the Algorithms 3 and 4 show. Additionally, the number of games executed by the RAN Slice Planner is equal to the number of RAN slices, thus a greater number of RAN slices may increase the number of iterations. In Table 3 we show the number of iterations performed by the RAN Slice Planner when a different number of cells, RBGs and RAN slices are considered. We observe the

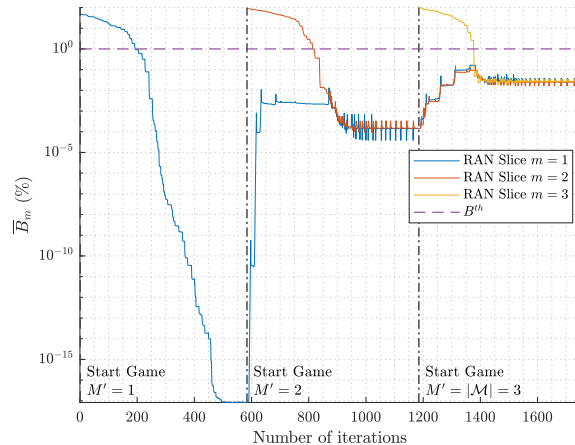


FIGURE 5. Evolution of the average UE blocking probabilities when the RAN Slice Planner executes the multiple ordinal potential games for $\mathcal{M} = 3$ RAN slices.

TABLE 3. Number of iterations performed by the RAN Slice Planner.

Number of cells $ \mathcal{Z} $	14	15	16	17	18
Considering: $ \mathcal{M} = 3$ RAN slices $W_i = 20$ MHz	665	702	993	1149	1356
Number of RAN slices $ \mathcal{M} $	1	2	3	4	5
Considering: $ \mathcal{Z} = 20$ cells $W_i = 20$ MHz	582	990	1299	2268	3450
Cell Bandwidth W_i	20 MHz	25 MHz	30 MHz	40 MHz	50 MHz
Considering: $ \mathcal{M} = 3$ RAN slices $ \mathcal{Z} = 20$ cells	1299	1365	1569	1869	2529

number of iterations grows exponentially when the number of RAN slices and RBGs (i.e., the cell bandwidth) increases. We also notice the number of iterations slightly increases when the number of cells increases.

C. COMPUTATIONAL COMPLEXITY ANALYSIS

We have also analyzed the execution time for a single iteration. This time mainly depends on the computation of (a) the PDFs of the average SINR, i.e., $f_{PDF}(\bar{\gamma}_u)$; and (b) the UE blocking probability $B_{i,m}$. Both are calculated for each pair of RAN slice and cell (see lines 10-11 in Algorithm 2). Regarding the time to compute the PDFs, it increases exponentially when the number of considered cells and RBGs available per cell increase. With respect to the time to compute the UE blocking probability, it increases exponentially when the amount of RBGs allocated for a RAN slice in a single cell increases (see [43, Section V.B]).

In this work, we have empirically estimated the statistical distribution of the execution time for a single iteration according to the number of cells, RAN slices and RBGs. Specifically, we have used box-and-whisker plots as Fig. 6 shows. For each plot, the bottom and the top of each box represent the first and third quartiles for the measured times, respectively, while the red line represents the 50th percentile. Focusing on the whiskers, the lowest and the highest lines represent the minimum and maximum measured times.

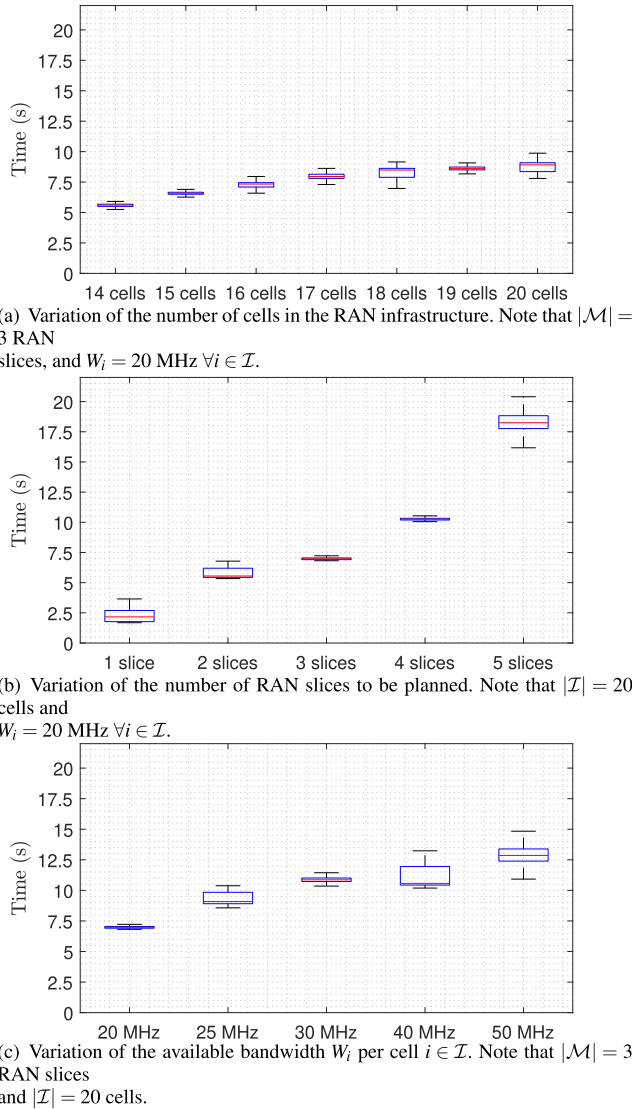


FIGURE 6. Statistical distribution of the execution time per iteration of the multiple ordinal potential games for different scenarios.

Focusing on Fig. 6(a), the execution time of an iteration slightly decreases when the number of cell decreases. In such a case, the RAN Slice Planner evaluates $|\mathcal{M}|$ PDFs and $|\mathcal{M}|$ UE blocking probabilities less per cell. The reduction of execution time is diminished by an increase of the required time to compute UE blocking probabilities. This is because the RAN Slice Planner tries to allocate more RBs to each RAN slice to meet its requirements. A similar behavior is observed in 6(b), where the increment of RAN slices involves computing more instances for the UE blocking probability. Specifically $|\mathcal{C}|$ instances for a new RAN slice. Finally, Fig. 6(c) shows how the time spent in an iteration increases when the available bandwidth increases in each cell. This is because a higher number of RBGs can be allocated for each RAN slice in each cell, taking more time to compute each UE blocking probability.

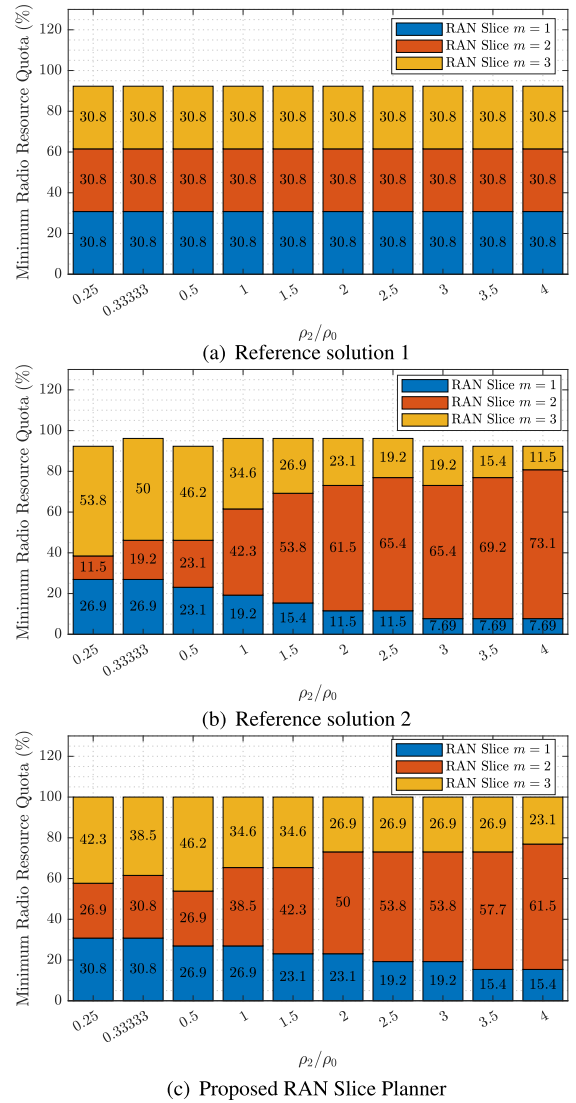


FIGURE 7. Minimum radio resource quotas computed in the cell $i = 18 \in \mathcal{C}$ (see Fig. 4). Note that $\rho_1 = \rho_3 = \rho_0$.

D. PERFORMANCE ANALYSIS

In this section, the performance of the RAN Slice Planner is compared with the reference solutions 1 and 2. In Fig. 7, we show the minimum radio resource quota computed for each RAN slice in a specific cell when the average offered traffic intensity of the RAN slice $m = 2$ differs from the remaining RAN slices, i.e., $\rho_2 \neq \rho_1$ and $\rho_2 \neq \rho_3$. Furthermore, Fig. 8 depicts the average UE blocking probability for the three RAN slices.

Focusing on the reference solution 1, the MNO under(over)-provisions radio resources for the three RAN slices because it always allocates them the same amount of radio resources regardless their traffic demands as Fig. 7(a) shows. If we observe Fig. 8, we notice RAN slice $m = 2$ has a significantly lower average UE blocking probability than the remaining RAN slices when ρ_2/ρ_0 is low. The

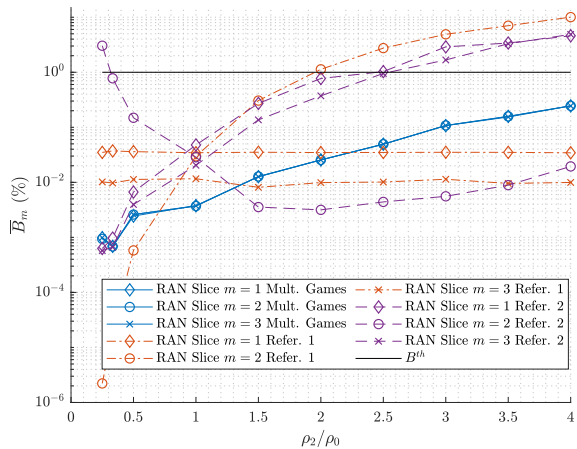
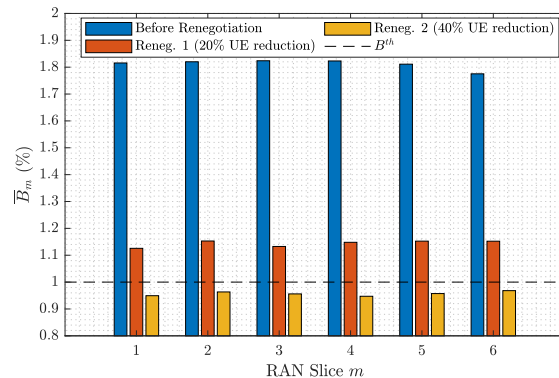


FIGURE 8. Evaluation of the average UE blocking probability \bar{B}_m per RAN slice when $\rho_1 = \rho_3 = \rho_0$ and ρ_2 takes different values.

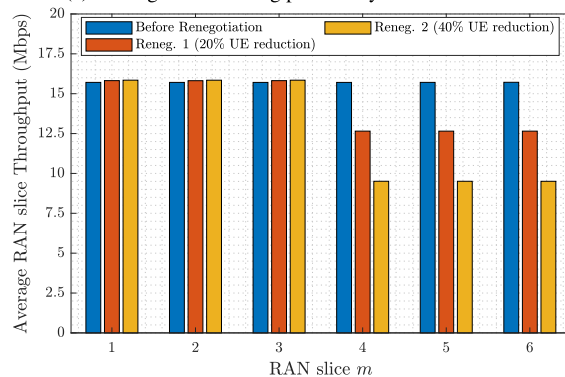
opposite happens for higher values of ρ_2/ρ_0 . This involves that (a) RAN slices $m = 1$ and $m = 3$ have higher values for the average UE blocking probability; and (b) the RAN slice $m = 2$ has not enough radio resources to achieve an average UE blocking probability below the imposed upper bound.

As Fig. 7(b) shows, the reference solution 2 determines the amount of radio resources allocated for the RAN slices in proportion to their average offered traffic intensities. This approach does not guarantee the average UE blocking probabilities are below the upper bound. This is mainly because the inter-cell interference levels are not considered neither to compute the radio resource quotas nor to translate these quotas into specific RBGs. We notice in Fig. 8 how the average UE blocking probability for RAN slice $m = 2$ is above the imposed upper bound for lower values of ρ_2/ρ_0 . We also observe a similar behavior for RAN slice $m = 1$ and $m = 3$ when ρ_2/ρ_0 is higher. This is because the reference solution 2 under-provisions radio resources for RAN slice $m = 2$ when ρ_2/ρ_0 is low, and over-provisions them for higher values of ρ_2/ρ_0 .

In the case of using the proposed RAN Slice Planner, we observe in Fig. 8 that our solution outperforms the reference solutions 1 and 2. Specifically, we notice the average UE blocking probabilities of all the RAN slices are practically the same and are always below the upper bound. The reason is our solution does not only consider the traffic demand and the average UE blocking probability for these RAN slices in each cell to allocate them radio resources, but also the inter-cell interference conditions in the RAN infrastructure. This means the RAN Slice Planner allocates more radio resources in a specific cell for those RAN slices i) which present a higher traffic demand and ii) whose UEs perceive a stronger interference from neighbor cells. An example of this situation is depicted in Fig. 7(c) for the RAN slice $m = 2$. This RAN slice receives more radio resources because it has the highest traffic demand in cell $i = 18$ and receives a stronger interference from RAN slice $m = 3$ in cells $i = 14$ and $i = 2$ (see Fig. 4).



(a) Average UE blocking probability for each RAN slice



(b) Effective Average Throughput for each RAN slice

FIGURE 9. RAN slice planning: (i) Before renegotiating the SLA, (ii) Renegotiation 1 (20% UE reduction); and (iii) Renegotiation 2 (40% UE reduction).

E. ANALYSIS OF THE RENEGOTIATION CAPABILITY

In this section, we have evaluated the renegotiation capability provided by the proposed RAN Slice Planner. To that end, we assume a scenario where (a) three RAN slices are currently running in the RAN and (b) the MNO receives the deployment requests of three new RAN slices. For simplicity, we consider all the RAN slices offer the same average traffic intensity and it is equal to the reference average traffic intensity $\rho_m = \rho_0$.

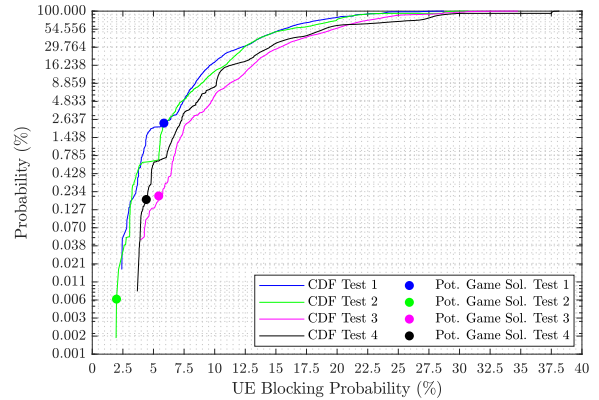
Under this scenario, the proposed RAN Slice Planner executes a planning procedure to determine if all the RAN slices can be accommodated into the RAN. This procedure results in the blue bars depicted in Fig.9(a). We notice the average UE blocking probability for all the RAN slices are above the imposed upper bound, thus the MNO cannot accommodate the six RAN slices. To solve that, the MNO should (a) renegotiate the SLA with the tenants which request the new RAN slices or (b) add more resources in the RAN infrastructure. In this experiment, we consider the MNO renegotiates the SLA with the tenants. Specifically, we assume the MNO negotiates a reduction in the number of subscribers for each RAN slice. This means the average offered traffic intensity for each new RAN slice is reduced. In the first renegotiation, the MNO reduces the available subscribers by a 20 %. This means $\rho_4 = \rho_5 = \rho_6 = 0.8\rho_0$. After the RAN Slice Planner re-executes the planning procedure, the average UE

blocking probability for each RAN slice (i.e., orange bars) is still above the upper bound despite the effective average throughput for the requested RAN slices is reduced as Fig. 9(b) shows. If this happens, the MNO tries to reduce more the amount of subscribers for the requested RAN slices. In the case of reducing the number of subscribers by a 40 % (i.e., $\rho_4 = \rho_5 = \rho_6 = 0.6\rho_0$) in these RAN slices, we observe (i.e., yellow bars) how the average UE blocking probability of each RAN slice is below the imposed upper bound.

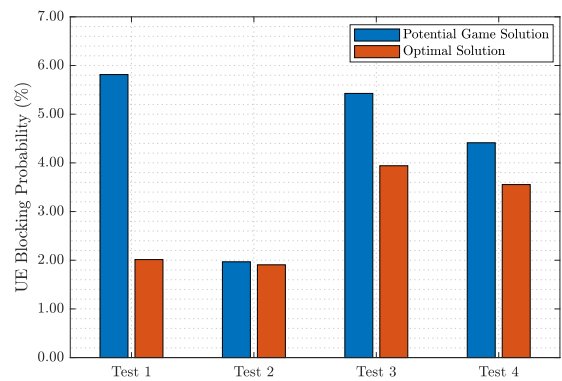
F. COMPARISON BETWEEN THE PROPOSED SOLUTION AND THE OPTIMAL SOLUTION

In the last experiment, we have compared how close is the solution obtained by the proposed RAN Slice Planer from the optimal solution. To that end, we have performed four tests, computing in each one (a) the sub-optimal solution obtained from our game-theoretic-based approach and (b) the values of the optimization function for the entire solution space by brute-force search. Due to the huge solution space in this problem, we have considered a small scenario to perform this experiment. Specifically, we have considered that 2 RAN slices must be deployed in 3 cells with 5 RBGs each one. Considering the MNO must allocate at least one RBG per cell and RAN slice, the number of possible solutions is around 6 millions. Based on this scenario, we have considered for each test that the RAN slices have different performance requirements in terms of GBR and UE density. Specifically: (test 1) RAN slice 1: $th_1 = 800$ Kbps and $\rho_1 = 0.6$, RAN slice 2: $th_1 = 600$ Kbps and $\rho_1 = 0.9$; (test 2) RAN slice 1: $th_1 = 450$ Kbps and $\rho_1 = 0.9$, RAN slice 2: $th_1 = 600$ Kbps and $\rho_1 = 0.6$; (test 3) RAN slice 1: $th_1 = 700$ Kbps and $\rho_1 = 0.9$, RAN slice 2: $th_1 = 500$ Kbps and $\rho_1 = 0.9$; and (test 4) RAN slice 1: $th_1 = 550$ Kbps and $\rho_1 = 0.9$, RAN slice 2: $th_1 = 650$ Kbps and $\rho_1 = 0.3$.

The results are depicted in Fig. 10. We show in Fig. 10(a) the Cumulative Distribution Function (CDF) for the values of the optimization function, considering the entire solution space by brute-force search, and for the four performed tests. We have also marked with a circle in each CDF the solution obtained by the proposed RAN slice Planner. We observe the worst case is presented in test 1, where the sub-optimal solution obtained by our game-theoretic-based approach is within the 2.5 % of best solutions. Despite the sub-optimal solution is not close enough to the optimum one (see Fig. 10(b)), we want to remark our approach got the sub-optimal solution in few seconds whereas the time spent to compute the optimal solution by brute-force search was approximately four days (unfeasible technique for large-scale problems). For the other tests, we obtained sub-optimal solutions closer to the optimum one. Specifically, in the test 4 we obtained a sub-optimal solution within the 0.006 % of best solutions. This means our approach can obtain solutions very close to the optimum one for some scenarios in a considerably reduced time if we compare the execution time of our approach with respect to the brute-force search.



(a) CDF for the values of Eq. (6), i.e., the optimization function, considering the entire solution space.



(b) Solution obtained by the proposed RAN Slice Planner vs the optimal solution.

FIGURE 10. Performance comparison between our game-theoretic-based solution and the optimal solution.

VIII. CONCLUSION AND FUTURE WORK

The RAN slice planning is a procedure to decide the feasibility of deploying new RAN slices over an existing RAN infrastructure and the configuration of such infrastructure accordingly. Despite its key importance, this procedure has barely explored in the literature. Instead, most of the existing solutions focus on a different procedure known as admission control. Despite their usefulness, they present some aspects which do not permit the MNO to use them as planning tools, e.g., one-by-one request processing, rejecting unfeasible requests instead of renegotiating the service level agreement, etc.

To address this knowledge gap, we propose a mathematical framework to compute the radio resource quotas which will guarantee the UE blocking probability for each RAN slice with GBR requirements is below an upper bound. We model the RAN slice planning using game theory. Specifically, we use multiple ordinal potential games and demonstrate the existence of a NE solution. To solve these games, we design novel strategies based on better response dynamics with the goal of minimizing the average UE blocking probability for

all the RAN slices. The simulation results demonstrate our solution allows the MNO to plan RAN slices in a scenario with resource scarcity whereas the reference solutions do not under the same conditions.

An interesting direction for future work extensions is the combination of GBR RAN slices with RAN slices with stringent requirements in terms of latency. For the latter, the goal of the RAN Slice Planner would be the derivation of the radio resource quotas which guarantee that a given percentile (e.g., 95%) of the traffic demands would present a latency below a certain upper bound. Additionally, we will work in the improvement of the RAN Slice Planner implementation. Specifically, we will optimize the algorithm implementations, reducing the computational complexity of the proposed RAN Slice Planner.

REFERENCES

- O. Adamuz-Hinojosa, P. Muñoz, J. Ordóñez-Lucena, J. J. Ramos-Munoz, and J. M. Lopez-Soler, "Harmonizing 3GPP and NFV description models: Providing customized RAN slices in 5G networks," *IEEE Veh. Technol. Mag.*, vol. 14, no. 4, pp. 64–75, Dec. 2019.
- Management and Orchestration; Concepts, Use Cases and Requirements (Release 17)*, document TS 28530, V.17.3.0, 3GPP, Sep. 2022.
- O. Adamuz-Hinojosa, "Network slicing management for 5G radio access networks," Ph.D. thesis, Dept. Signal Theory, Telematics Commun., Univ. Granada, Granada, Spain, Apr. 2022. [Online]. Available: <https://digibug.ugr.es/handle/10481/74957>
- P. Muñoz, O. Sallent, and J. Pérez-Romero, "Self-dimensioning and planning of small cell capacity in multitenant 5G networks," *IEEE Trans. Veh. Technol.*, vol. 67, no. 5, pp. 4552–4564, May 2018.
- F. Bahlke, O. D. Ramos-Cantor, S. Henneberger, and M. Pesavento, "Optimized cell planning for network slicing in heterogeneous wireless communication networks," *IEEE Commun. Lett.*, vol. 22, no. 8, pp. 1676–1679, Aug. 2018.
- O. Al-Khatib, W. Hardjawana, and B. Vucetic, "Spectrum sharing in multitenant 5G cellular networks: Modeling and planning," *IEEE Access*, vol. 7, pp. 1602–1616, 2019.
- P. Muñoz, Ñ. Adamuz-Hinojosa, J. Navarro-Ortiz, O. Sallent, and J. Pérez-Romero, "Radio access network slicing strategies at spectrum planning level in 5G and beyond," *IEEE Access*, vol. 8, pp. 79604–79618, 2020.
- Q.-T. Luu, S. Kerboeuf, and M. Kieffer, "Admission control and resource reservation for prioritized slice requests with guaranteed SLA under uncertainties," *IEEE Trans. Netw. Serv. Manag.*, vol. 19, no. 3, pp. 3136–3153, Sep. 2022.
- J. Zheng, P. Caballero, G. de Veciana, S. J. Baek, and A. Banchs, "Statistical multiplexing and traffic shaping games for network slicing," *IEEE/ACM Trans. Netw.*, vol. 26, no. 6, pp. 2528–2541, Dec. 2018.
- B. Han, D. Feng, and H. D. Schotten, "A Markov model of slice admission control," *IEEE Netw. Lett.*, vol. 1, no. 1, pp. 2–5, Mar. 2019.
- D. Bega, M. Gramaglia, A. Banchs, V. Sciancalepore, and X. Costa-Perez, "A machine learning approach to 5G infrastructure market optimization," *IEEE Trans. Mobile Comput.*, vol. 19, no. 3, pp. 498–512, Mar. 2020.
- B. Han, J. Lianghai, and H. D. Schotten, "Slice as an evolutionary service: Genetic optimization for inter-slice resource management in 5G networks," *IEEE Access*, vol. 6, pp. 33137–33147, 2018.
- M. J. Osborne and A. Rubinstein, *A course in Game Theory*. Cambridge, MA, USA: MIT Press, 1994.
- V. Sciancalepore, X. Costa-Perez, and A. Banchs, "RL-NSB: Reinforcement learning-based 5G network slice broker," *IEEE/ACM Trans. Netw.*, vol. 27, no. 4, pp. 1543–1557, Aug. 2019.
- B. Han, V. Sciancalepore, X. Costa-Perez, D. Feng, and H. D. Schotten, "Multiservice-based network slicing orchestration with impatient tenants," *IEEE Trans. Wireless Commun.*, vol. 19, no. 7, pp. 5010–5024, Jul. 2020.
- M. Vincenzi, E. Lopez-Aguilera, and E. Garcia-Villegas, "Maximizing infrastructure providers' revenue through network slicing in 5G," *IEEE Access*, vol. 7, pp. 128283–128297, 2019.
- J. Prados-Garzon, A. Laghrissi, M. Bagaa, T. Taleb, and J. M. Lopez-Soler, "A complete LTE mathematical framework for the network slice planning of the EPC," *IEEE Trans. Mobile Comput.*, vol. 19, no. 1, pp. 1–14, Jan. 2020.
- B. Xiang, J. Elias, F. Martignon, and E. Di Nitto, "Joint planning of network slicing and mobile edge computing: Models and algorithms," 2020, *arXiv:2005.07301*.
- J. Perez-Romero and O. Sallent, "Optimization of multitenant radio admission control through a semi-Markov decision process," *IEEE Trans. Veh. Technol.*, vol. 69, no. 1, pp. 862–875, Jan. 2020.
- I. Vilà, O. Sallent, A. Umbert, and J. Pérez-Romero, "An analytical model for multi-tenant radio access networks supporting guaranteed bit rate services," *IEEE Access*, vol. 7, pp. 57651–57662, 2019.
- P. Caballero, A. Banchs, G. de Veciana, X. Costa-Pérez, and A. Azcorra, "Network slicing for guaranteed rate services: Admission control and resource allocation games," *IEEE Trans. Wireless Commun.*, vol. 17, no. 10, pp. 6419–6432, Oct. 2018.
- P. Caballero, A. Banchs, G. de Veciana, and X. Costa-Pérez, "Multi-tenant radio access network slicing: Statistical multiplexing of spatial loads," *IEEE/ACM Trans. Netw.*, vol. 25, no. 5, pp. 3044–3058, Dec. 2017.
- P. Caballero, A. Banchs, G. De Veciana, and X. Costa-Pérez, "Network slicing games: Enabling customization in multi-tenant mobile networks," *IEEE/ACM Trans. Netw.*, vol. 27, no. 2, pp. 662–675, Apr. 2019.
- D. H. Kim, S. M. A. Kazmi, A. Ndikumana, A. Manzoor, W. Saad, and C. S. Hong, "Distributed radio slice allocation in wireless network virtualization: Matching theory meets auctions," *IEEE Access*, vol. 8, pp. 73494–73507, 2020.
- S. Zazo, S. Valcarcel Macua, M. Sanchez-Fernandez, and J. Zazo, "Dynamic potential games with constraints: Fundamentals and applications in communications," *IEEE Trans. Signal Process.*, vol. 64, no. 14, pp. 3806–3821, Jul. 2016.
- D. D. Penda, A. Abrardo, M. Moretti, and M. Johansson, "Distributed channel allocation for D2D-enabled 5G networks using potential games," *IEEE Access*, vol. 7, pp. 11195–11208, 2019.
- Management and Orchestration; 5G Network Resource Model (NRM); Stage 2 and Stage 3 (Release 17)*, document TS 28541, V.17.0.0, 3GPP, Sep. 2020.
- Management and Orchestration; Architecture Framework (Release 16)*, document TS 28533, V.16.5.0, 3GPP, Mar. 2020.
- Generic Network Slice Template (Version 3.0)*, GSM Association, London, U.K., May 2020.
- I. Afolabi, T. Taleb, K. Samdanis, A. Ksentini, and H. Flinck, "Network slicing and softwarization: A survey on principles, enabling technologies, and solutions," *IEEE Commun. Surveys Tuts.*, vol. 20, no. 3, pp. 2429–2453, 3rd Quart., 2018.
- T. Guo and A. Suárez, "Enabling 5G RAN slicing with EDF slice scheduling," *IEEE Trans. Veh. Technol.*, vol. 68, no. 3, pp. 2865–2877, Mar. 2019.
- R. Ferrus, O. Sallent, J. Perez-Romero, and R. Agustí, "On the automation of RAN slicing provisioning and cell planning in NG-RAN," in *Proc. Eur. Conf. Netw. Commun. (EuCNC)*, Jun. 2018, pp. 37–42.
- Management and Orchestration; Provisioning; (Release 16)*, document TS 28531, V.16.7.0, 3GPP, Sep. 2020.
- J. Ordóñez-Lucena, P. Ameigeiras, L. M. Contreras, J. Folgueira, and D. R. López, "On the rollout of network slicing in carrier networks: A technology radar," *Sensors*, vol. 21, no. 23, p. 8094, 2021.
- NR; User Equipment (UE) Radio Access Capabilities (Release 16)*, document TS 38.306 V.16.2.0, 3GPP, Oct. 2019.
- User Equipment (UE) Radio Transmission and Reception; Part 1: Range 1 Standalone (Release 16)*, document TS 38.101-1, V.16.3.0, 3GPP, Mar. 2020.
- User Equipment (UE) Radio Transmission and Reception; Part 2: Range 2 Standalone (Release 16)*, document TS 38.101-2, V.16.4.0, 3GPP, Jun. 2020.
- NR, Physical Channels and Modulation (Release 16)*, document TS 38.211, V.16.2.0, 3GPP, Jun. 2020.
- NR, Physical Layer Procedures for Data (Release 16)*, document TS 38.214, V.16.1.0, 3GPP, Mar. 2020.
- Study on New Radio Access Technology: Radio Frequency (RF) and Co-Existence Aspects (Release 14)*, document TR 38.803, V.14.2.0, 3GPP, Sep. 2017.
- L. Kleinrock, *Queue Systems*, vol. 1. Hoboken, NJ, USA: Wiley, 1975.
- V. B. Iversen, "Teletraffic engineering and network planning," DTU Fotonik, Lyngby, Denmark, Tech. Rep., 2015. [Online]. Available: <https://orbit.dtu.dk/en/publications/teletraffic-engineeringandnetwork-planning>

- [43] O. Adamuz-Hinojosa, P. Ameigeiras, P. Munoz, and J. Lopez-Soler, "Analytical model for the UE blocking probability in an OFDMA cell providing GBR slices," in *Proc. IEEE Wireless Commun. Netw. Conf. (WCNC)*, Nanjing, China, Mar. 2020, pp. 1–7.
- [44] D. Bauso, *Game Theory With Engineering Applications*. Philadelphia, PA, USA: SIAM, 2016.
- [45] Y. H. Chew, Q. D. Lă, and Y. H. Chew, *Potential Game Theory: Applications in Radio Resource Allocation*. Cham, Switzerland: Springer, 2016.
- [46] M. Feldman, Y. Snappir, and T. Tamir, "The efficiency of best-response dynamics," in *Proc. Int. Symp. Algorithmic Game Theory*. L'Aquila, Italy: Springer, 2017, pp. 186–198. [Online]. Available: <https://cs.gssi.it/sagt2017/>
- [47] *Study on Channel Model for Frequencies From 0.5 to 100 GHz (Release 16)*, document TS 38.901, V.16.1.0, 3GPP, Dec. 2019.



slicing in beyond 5G/6G and radio access networks (RAN).

OSCAR ADAMUZ-HINOJOSA received the B.Sc., M.Sc., and Ph.D. degrees in telecommunications engineering from the University of Granada, Spain, in 2015, 2017, and 2022, respectively. He was granted a Ph.D. fellowship by the Education Spanish Ministry, in September 2018. He is currently working as an Interim Assistant Professor with the Department of Signal Theory, Telematics and Communication, University of Granada. His research interests include network



access network planning and management, application of artificial intelligence tools in radio resource management, and virtualization of wireless networks.

PABLO MUÑOZ received the M.Sc. and Ph.D. degrees in telecommunication engineering from the University of Málaga, Málaga, Spain, in 2008 and 2013, respectively. He is currently an Assistant Professor with the Department of Signal Theory, Telematics, and Communications, University of Granada, Granada, Spain. He has published more than 50 articles in peer-reviewed journals and conferences. He is the coauthor of four international patents. His research interests include radio



5G and the IoT technologies.

PABLO AMEIGEIRAS received the M.Sc. degree in electrical engineering from the University of Malaga, Spain, in 1999. He performed his master's thesis at the Chair of Communication Networks, Aachen University, Germany. In 2000, he joined Aalborg University, Denmark, where he carried out his Ph.D. thesis. In 2006, he joined the University of Granada, where he has been leading several projects in the field of LTE and LTE Advanced Systems. His currently research interests include



design and modeling of beyond 5G and 6G.

JUAN M. LOPEZ-SOLER received the B.Sc. degree in physics (electronics) and the Ph.D. degree from the University of Granada, in 1987 and 1995, respectively. He is currently a Full Professor with the Department of Signals, Telematics and Communications, University of Granada. Since 2012, he has directed the Wireless and Multimedia Networking (WiMunet) Laboratory, University of Granada. He has participated in 23 research projects with public funding and 17 private ones (leading 18 of them). He has advised eight Ph.D. thesis, published 33 articles in indexed journals, and contributed to more than 45 workshops/conferences. His current research interests include network

...